An Equation of State for the Self-Diffusion Coefficient in Lennard–Jones Fluid Derived by Molecular Dynamics Simulations

Yosuke Kataoka* **and Minoru Fujita†**

Department of Materials Chemistry, College of Engineering, Hosei University, 3-7-2 Kajinocho, Koganei, Tokyo 184

†Graduate School of Engineering, Hosei University, 3-7-2 Kajinocho, Koganei, Tokyo 184

(Received July 22, 1994)

The self-diffusion coefficient in Lennard–Jones fluid was studied by molecular dynamics simulation. Simulations were done at 414 states in the temperature–volume plane. An equation of state for the self-diffusion coefficient was derived by the least-square fitting. The calculated equation of state was in agreement with the experimental results on CO_2. Its pressure dependence was also consistent with that in liquid hexane. The liquid structure was analyzed by the excess coordination number, the distributions of the cluster size and the hole volume. The volume dependence of the self-diffusion coefficient in the two-phase region was discussed in terms of the coordination number in the first shell.

The molecular dynamics (MD) simulations are used to study the dynamical properties in fluids.[1] Some equations of state are reported for the pressure–volume–temperature relation in a Lennard–Jones fluid.[2—6] As far as we know, no equations of state for the self-diffusion coefficient have been obtained by MD. Such an equation can be used for a comparison with the experimental results. Our naive question is whether the liquid–gas critical point has a special meaning in the equation of state for the self-diffusion coefficient. The equation can be used as the base line in the analysis of the self-diffusion coefficient near the critical point where some anomaly is expected.

We are going to obtain the self-diffusion coefficient in a system with 108 Lennard–Jones molecules. Some simulations on the system with the 864 molecules will be carried out for a comparison. The rather small 108 system is sufficient for the present aim to derive the equation of state for the self-diffusion coefficient.

Once the simulations in the wide temperature–volume space were performed, the least square fitting is applied to obtain the equation of state (EOS). The result will be compared with the experiments.[7—9] It is also compared with the theory.[10,11]

The liquid structure will be studied in the next section. The temperature and volume dependence will be described for the excess coordination number and the distributions of the size of the cluster and the volume of the hole.

In the last section we will get some relation between the self-diffusion coefficient and the coordination number in the first shell. The fluctuation in density is most important in this analysis. Large fluctuations in density are expected near the critical point. The self-diffusion coefficient will suffer. However, such events will occur in the sufficiently large system. We analyze the small samples at low temperatures to see a similar effect of the fluctuation in density. At this temperature most of the volume corresponds to the two-phase region, where the molecules tend to separate into the liquid and gas phases. Because our system is so small and our MD simulation is not very long, the phase separation is far from complete in most of the volume. For this reason, such samples are used in the analysis.

Method of Simulation

The Lennard–Jones potential is assumed:

$$\phi(r) = 4\varepsilon\left(\left(\frac{\sigma}{r}\right)^{12} - \left(\frac{\sigma}{r}\right)^{6}\right). \tag{1}$$

The program calculates the time evolution of the system using a predictor-corrector algorithm.[1] The temperature is controlled by Nosé's method.[12,13] The periodic boundary condition is assumed in the cubic cell. The force is cut off at the half of the MD cell width.

The unit of time τ is defined as follows

$$\tau = \sigma\sqrt{\frac{m}{\varepsilon}}, \tag{2}$$

Where m is the mass of the molecule. The time step is

$$\mathrm{d}t = 0.0023\tau, \tag{3}$$

at most temperatures.

The following reduced quantities are used in this paper. The volume V of the system with the N molecules is written in units of $N\sigma^3$:

$$V_r = \frac{V}{N\sigma^3}. \quad (4)$$

The temperature T is reduced by the energy parameter ε and the Boltzmann constant k:

$$T_r = \frac{T}{\frac{\varepsilon}{k}}. \quad (5)$$

The pressure P is expressed in units of ε/σ^3:

$$P_r = \frac{P}{\frac{\varepsilon}{\sigma^3}}. \quad (6)$$

The time t is measured by the time unit defined in Eq. 2:

$$t_r = \frac{t}{\tau}. \quad (7)$$

As a result the self-diffusion coefficient D_r is reduced by σ^2/τ:

$$D_r = \frac{D}{\frac{\sigma^2}{\tau}}. \quad (8)$$

In our standard calculation, an 10000-step run is performed. In the gas state, a 50000 or 100000-step run was needed to obtain the self-diffusion coefficient. At each volume a random configuration is first obtained and the MD simulation at very high temperatures is performed. Then this sample is cooled gradually at the same volume.

The self-diffusion coefficient was calculated from the plot of the mean square displacement as a function of time.[1] In Fig. 1 the self-diffusion coefficient D_r of the system with 108 molecules in the unit cell is compared with that of a 864-molecule system. Our results are in good agreement with those of Levesque and Verlet.[14] The smaller system is sufficient to obtain the self-diffusion coefficient at more temperatures, although some differences are seen at the lowest temperatures (0.90).

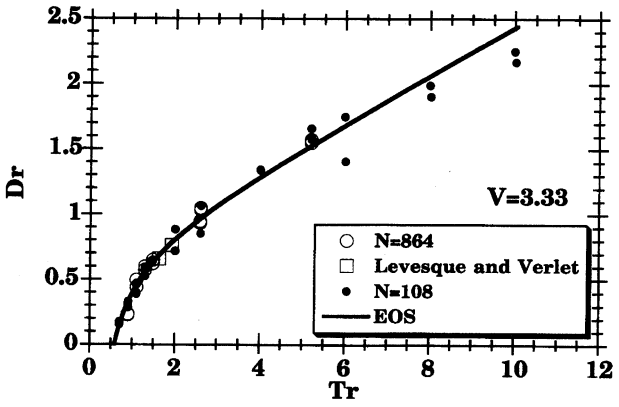

Fig. 1. The self diffusion coefficient D_r versus temperature T_r plot, at volume V_r=3.33. The number of the molecules in the unit cell is N. The square means the result by Levesque and Verlet (Ref. 14), where the number in the unit cell N is 864.

The simulated 12×22=264 states cover a wide region, as follows: the 12 temperatures T_r are selected from 0.70 to 10 and the 22 volumes V_r from 0.833 to 1000. The 150 states around the dense liquid states are chosen from the 10×20=200 states: the 10 temperatures T_r from 0.54 to 1.30 and the 20 volumes V_r from 1.00 to 1.40. The total number of the state accessed is 414. The simulation was repeated twice at each state. These states are shown in Fig. 2. This shows that the typical fluid states are covered in the present study. Some examples of the pressure P_r versus volume $V_r$curve at constant temperature T_r are described in Fig. 3. This is consistent with the EOS for P–V–T derived previously.[4] The critical temperature T_{cr} is 1.35 and the critical volume V_{cr} is 2.9.[4]

Equation of State for Self-Diffusion Coefficient

The self-diffusion coefficient D_r increases as a function of temperature T_r at constant volume V_r as shown in Fig. 4. Figure 5 describes the volume-variation of $D_r$at several temperatures. Although D_r itself is a steep function, the quantity $D_r/(V_r T_r)$ is moderate as a function of temperature and volume. For this reason this form is used in the least square fitting of the observed D_r.

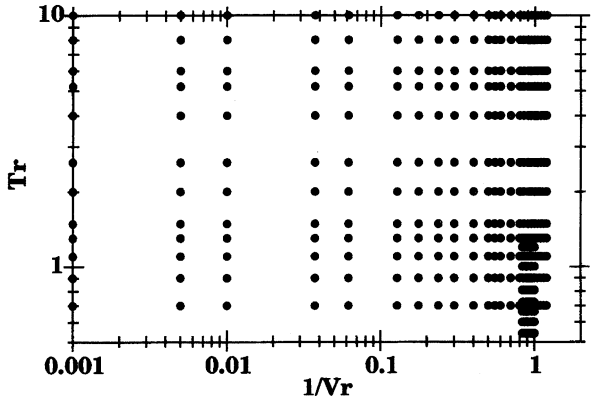

Fig. 2. The map of state points simulated.

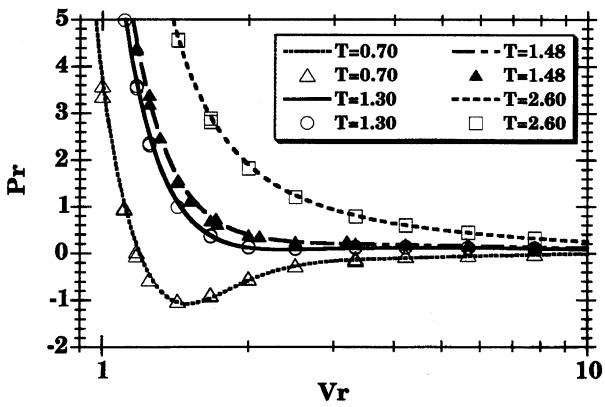

Fig. 3. The pressure P_r versus volume V_r at several given temperatures T_r. The dots are the simulated results and the curves are fitted ones.

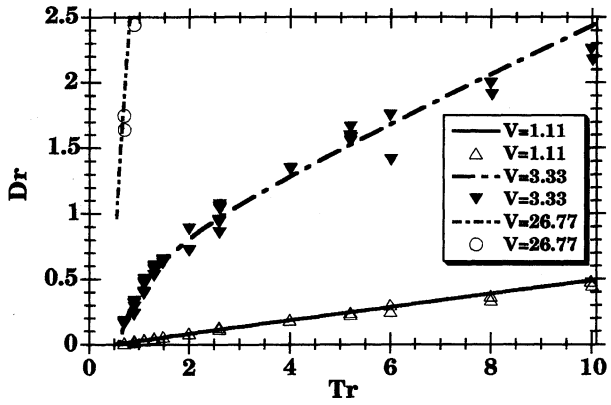

Fig. 4. The self diffusion coefficient D_r versus temperature T_r plot, at several volumes V_r. The marks are the MD values and the curves are EOS.

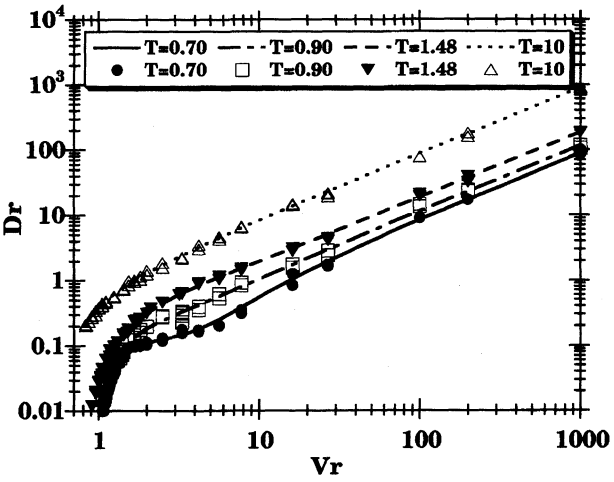

Fig. 5. The self diffusion coefficient D_r versus volume V_r plot, at several temperatures T_r. The marks are the MD results and the curves are EOS.

$$\frac{D_r}{V_r T_r} = \sum_{p=0,1,2,3}^{4} \sum_{q=0,1,2}^{3} A_{pq} \left(\frac{1}{V_r}\right)^p \left(\frac{1}{T_r}\right)^q, \tag{9}$$

$$p=0,1,2,3,4,$$
$$q=0,1,2,3. \tag{10}$$

The values of the 20 coefficients A_{pq} are listed in Table 1. The total number of the data points is 846. The relative deviation is obtained as follows:

$$\frac{\langle[\delta\left(\frac{D_r}{V_r T_r}\right)]^2\rangle^{1/2}}{\langle\left(\frac{D_r}{V_r T_r}\right)^2\rangle^{1/2}} = 0.087. \tag{11}$$

Some examples of the fitting are shown in Figs. 4 and 5.

Comparison with CO_2 Data. The self-diffusion coefficient of CO_2 is measured as a function of density at 25 and 42 °C (Fig. 6).[7,8] For a comparison, we use the following potential parameters:[10]

$$\sigma=0.3941 \text{ nm},$$
$$\frac{\varepsilon}{k}=195.2 \text{ K}. \tag{12}$$

Table 1. Coefficient A_{pq} in the Equation of State

p	q	A_{pq}
0	0	0.0773629
0	1	0.1235587
0	2	−0.0925246
0	3	0.0214779
1	0	−0.1478025
1	1	0.9364020
1	2	−0.7624413
1	3	−0.1248177
2	0	0.3122186
2	1	−2.9629708
2	2	2.8495073
2	3	0.2425943
3	0	−0.2779113
3	1	2.6573926
3	2	−3.1006457
3	3	−0.1919803
4	0	0.0776658
4	1	−0.7898671
4	2	1.1050118
4	3	0.0563687

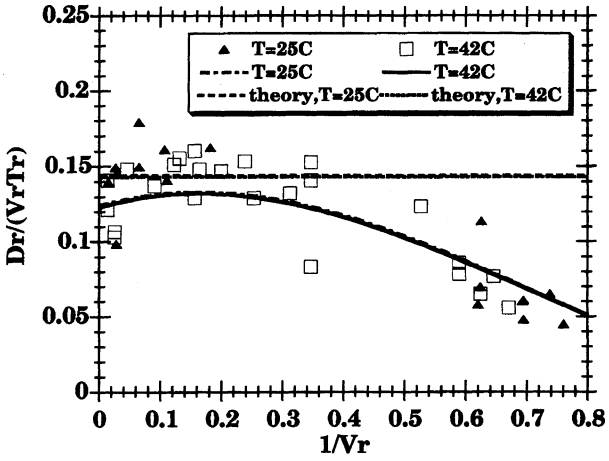

Fig. 6. Plot of $D_r/(V_r T_r)$ against density $1/V_r$ at 25 and 42 °C for CO_2. The dots are the experimental results[7,8] and the curves are EOS. Theory is Eq. 14.

The unit for the self-diffusion coefficient is

$$\frac{\sigma^2}{\tau} = 7.57 \times 10^{-4} \text{cm}^2 \text{s}^{-1}. \tag{13}$$

Two curves at 25 and 42 °C sit almost at the same place because of their weak temperature dependence. We see that the calculated values are in good agreement with the experimental ones.

The theoretical result from solving the Boltzmann equation is also compared with the present calculations in Fig. 6. The Chapman and Enskog theory gives the following equation:[10]

$$D = \frac{3}{16} \frac{\left(\frac{4\pi kT}{m}\right)^{1/2}}{n\pi\sigma^2\Omega_D}. \tag{14}$$

Here n is the number density and Ω_D is the diffusion collision integral. This is a function of temperature and

does not depend on the density. It is given by Neufeld et al.[11] The theoretical lines of $D_r/(V_r T_r)$ do not depend on the volume, as seen from Eq. 14. These depend on the temperature weakly. As this is a collision theory, it deviates from the observed results in the dense region.

Comparison with Hexane. It is known that the self-diffusion coefficient of hexane has this pressure dependence:[9,10]

$$\ln D = a + bP^{0.75}, \tag{15}$$

at low temperatures in the dense liquid region. Here a and b are constants. A similar plot is shown in Fig. 7, where the equation of state for the pressure–volume–temperature relation[4] is used. The empirical equation (Eq. 15) is consistent also in a Lennard–Jones liquid at $T_r \leq 1.10$.

Temperature and Density Variation of D. The temperature dependence of the quantity $D_r/(V_r T_r)$ is depicted in Fig. 8. Figure 9 describes its density variation. From Fig. 8 it is seen that $D_r/(V_r T_r)$ has a maximum around $T_r = 1.4$, is about the critical temperature ($T_{cr} = 1.35$).[4] Figure 9 shows that $D_r/(V_r T_r)$ is maximum around $V_r = 6.3$ and its ratio to the critical volume[4] is $6.3/V_{cr} = 6.3/2.9 = 2.2$. In the present equation of state (Eq. 9) the critical point is not a singular point. In the case of the observed CO_2 fluid in Fig. 6, no singularities appear at these temperatures. The critical temperature is 31 °C and the critical density is 0.39 σ^{-3}. The anomaly may be seen in the very narrow region around the critical point in the real system. We cannot expect such an effect to appear in a small system.

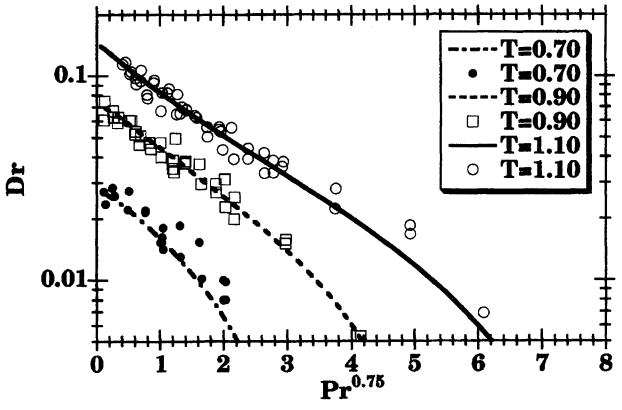

Fig. 7. The self diffusion coefficient D_r versus pressure $P_r^{0.75}$ plot, at several temperatures T_r. The marks are the MD results and the curves are EOS.

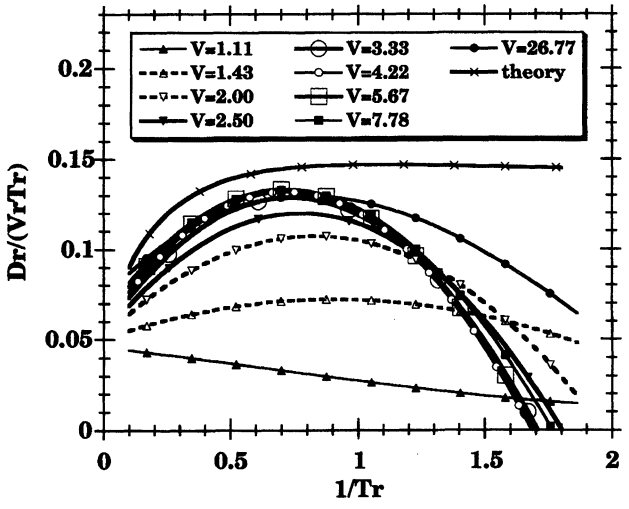

Fig. 8. Plot of $D_r/(V_r T_r)$ against inverse of temperature $1/T_r$ at several volumes V_r, EOS.

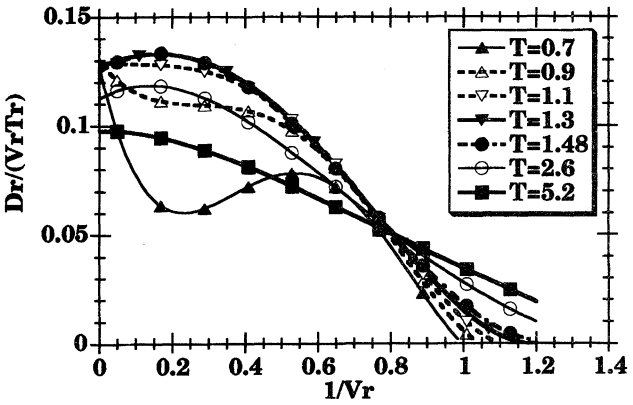

Fig. 9. Plot of $D_r/(V_r T_r)$ versus density $1/V_r$ at several temperatures T_r, EOS.

The theoretical results are also shown in Fig. 8. They have no volume dependence. They are consistent with the obtained equation of state in the low density limit.

Liquid Structure as a Function of T and V

In this section the structure in liquid is studied. We expect it to have a large influence on the self-diffusion coefficient.

Excess Coordination Number. The structure in liquid is usually discussed by the radial distribution function $g(R)$. In the present study we calculate the deviation of the local density from the average distribution. The average number density is ρ_o. The excess distribution function at the distance R is written below:

$$\Delta\rho(R) = 4\pi\rho_o R^2\{g(R) - 1\}. \tag{16}$$

The excess coordination number (ECN) in the region up to the molecular distance R is the running sum of $\Delta\rho(R)$:

$$\mathrm{ECN}(R) = \int_0^R \Delta\rho(R')\mathrm{d}R'. \tag{17}$$

An example is shown in Fig. 10. This is a case with large deviation from the average. We use the minimum image method to find a neighbor in the simulation.[1] For this reason, the molecular distance has a maximum value $0.5L3^{1/2}$, where L is the length of the unit cell. Because of the periodic boundary conditions, ECN must be zero at this distance. In Fig. 10, ECN is maximum around $R_r = 4$. Hereafter ECN(R_r=3.5) is discussed.

The ECN is plotted as a function of temperature and

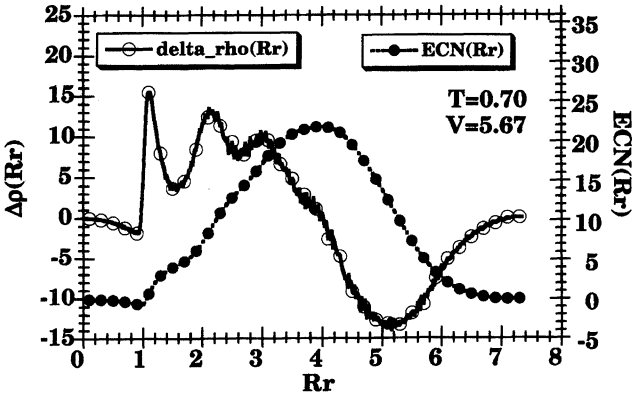

Fig. 10. The excess distribution function $\Delta\rho(R_r)$ and the excess coordination number ECN(R_r) versus the molecular distance R_r at T_r=0.70 and V_r=5.67, see Eqs. 16 and 17.

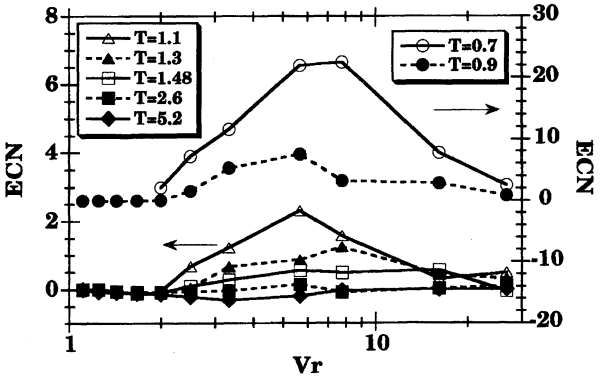

Fig. 11. The excess coordination number (ECN) at R_r=3.5 versus volume V_r plot, at several temperatures T_r.

volume in Fig. 11. It has a maximum around V_r=5−8, which is a little larger than the critical volume V_{cr}=2.9. The maximum value is only 1.2 around the critical temperature T_{cr}=1.35, although it depends on the system size. At lower temperatures, the states with the volume around 3—10 correspond to the two-phase region.[4] However, the degree of the phase separation is not so large, as is also seen from the van der Waals loop in Fig. 3. The ECN in Fig. 11 shows that the phase separation continues gradually as the temperature decreases. This comes from the length of the run in the present MD simulation. The present runs were not long enough to complete the phase separation in the two-phase region. As the samples at low temperatures were obtained by the cooling process, the configurations at low temperatures include the well-mixed ones at high temperatures. For this reason, the calculated result in the two-phase region is only an example of the configurations with large density fluctuations.

Distribution of the Cluster Size. Another method to examine the structure in the liquid is through the statistics on the cluster size. Here a cluster is defined as the set of connected molecules where two molecules within the distance 1.6σ are called connected.

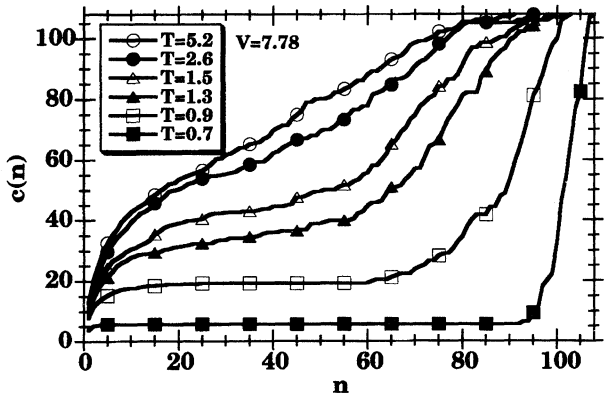

Fig. 12. The running sum $c(n)$ of the distribution function of the cluster size $f_{cl}(n)$ up to size n is plotted against n at several temperatures T_r, V_r=7.78.

The size of cluster means the number of molecules in the cluster. The distribution function of the cluster size n is written as $f_{cl}(n)$. The running sum $c(n)$ up to n is plotted against n in Fig. 12.

$$c(n) = \sum_{n'=0,1,2,}^{n} n' f_{cl}(n'). \tag{18}$$

Figure 12 describes the case V_r=7.78. The distributions at several temperatures are compared. The $c(n)$ curve means there are many clusters around steep increasing part. From this figure we see that there is a broad distribution at high temperatures. There are clusters less than 5 and from 60—100 at T_r=1.30 near the critical temperature. At low temperatures, most of the clusters are larger than 95.

The volume dependence in $c(n)$ at low temperatures (T_r=7.0) is shown in Fig. 13. The distribution of the cluster at V_r=3.33, 5.67, and 7.78 is localized around 100. In the contrast to this, there are peaks around less than 10 and between 55—75 in the distribution at V_r=16.17. This means that there are liquid-likes part and gas-like ones in the sample (T_r=0.70, V_r=16.17).

Distribution of Hole Volume. The open space which the molecules do not occupy is called a hole. The distribution of the volume of the holes is also useful

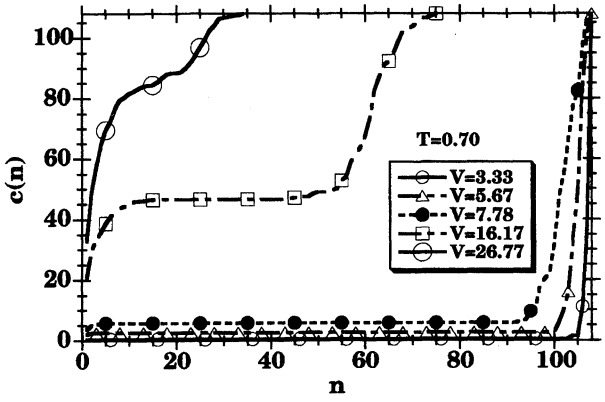

Fig. 13. The running sum $c(n)$ versus n plot at several volumes V_r, T_r=0.70.

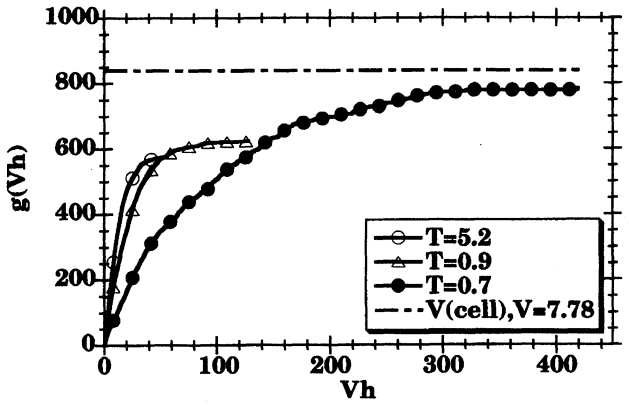

Fig. 14. The running sum $g(V_h)$ of the distribution function of the hole volume $f_h(V_h)$ up to volume V_h is plotted against V_h at several temperatures T_r, V_r=7.78. The units of V_h and $g(V_h)$ are σ^3. The straight line is the volume of the unit cell.

information to specify the liquid structure.

The holes are searched for at the lattice points. The mesh size of the lattice points is 1/40 of the cell length. The radius of the molecule is assumed as $\sigma/2$. In a given configuration of molecules, the largest sphere which does not overlap any molecules is first found. Then the largest sphere which does not overlap any molecules and spheres is searched for next. This process is repeated until the new sphere is small enough. The two touching spheres are defined as belonging to the same hole. The volume of the hole h_i is the sum of the volumes of the spheres in the hole:

$$V_h(h_i) = \sum_{r \in hi} \frac{4}{3}\pi r^3, \tag{19}$$

Where r is the radius of the sphere.

The distribution of the volume V_h of the hole is written as $f_h(V_h)$. The running sum $g(V_h)$ of $f_h(V_h)$ is plotted at V_r=7.78 in Fig. 14.

$$g(V_h) = \int_0^{V_h} V_h' f_h(V_h') \mathrm{d}V_h'. \tag{20}$$

At high temperature (T_r=5.2), the volume of the hole

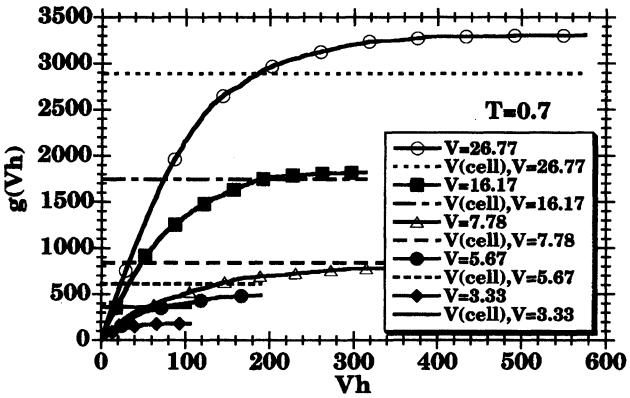

Fig. 15. The running sum $g(V_h)$ versus V_h plot at several volumes V_r, T_r=0.70.

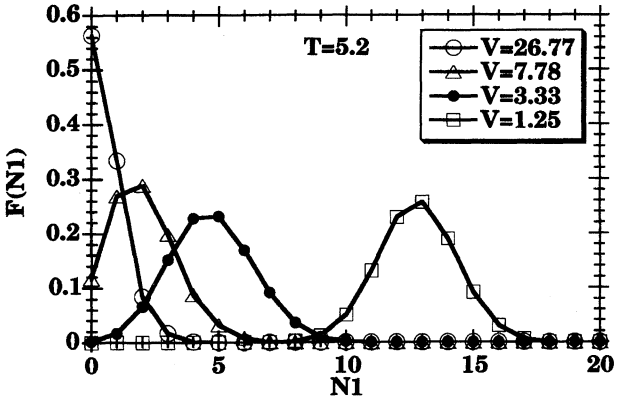

Fig. 16. The distribution functions $F(N1)$ of the first coordination number $N1$ at several volumes V_r, T_r= 5.2.

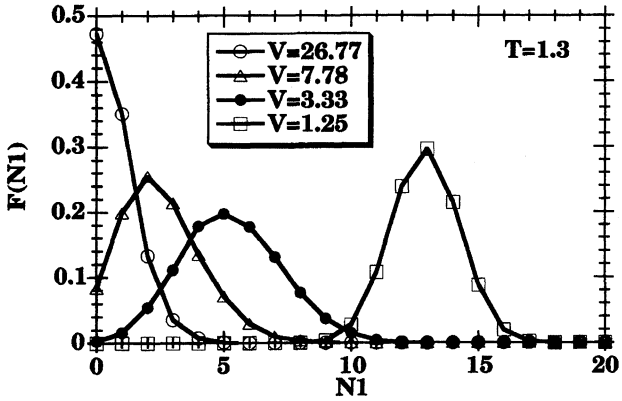

Fig. 17. The distribution functions $F(N1)$ at several volumes V_r, T_r=1.3.

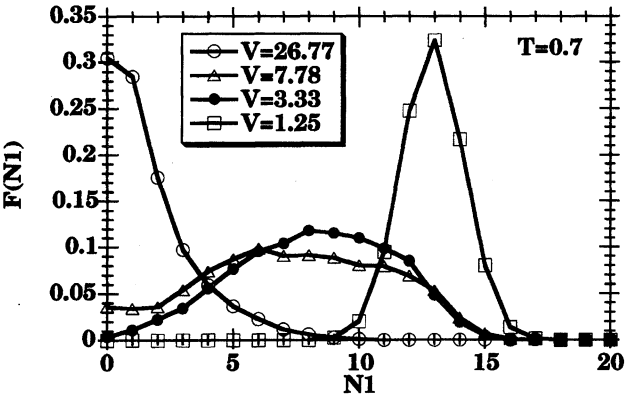

Fig. 18. The distribution functions $F(N1)$ at several volumes V_r, T_r=0.7.

is less than 20. (The units of V_h and $g(V_h)$ are σ^3). The total sum of it is 580, where the volume of the unit cell is 850. The space occupied by the molecules is $108\times(4/3)\pi(\sigma/2)^3=56.5\sigma^3$. These values and Figs. 11 and 12 mean that the molecular distribution is random at high temperatures. The distribution of the volume of the hole changes only a little until low temperature (0.90) at V_r=7.78. At the lowest temperature 0.70, there are peaks around 20, 100, and 250 in the distribu-

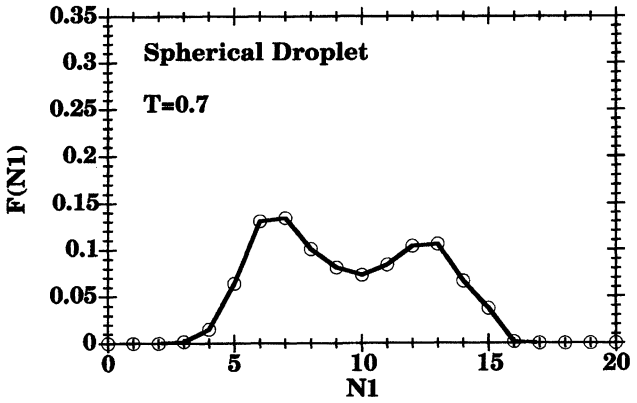

Fig. 19. The distribution functions $F(N1)$ of the first coordination number $N1$ in a case of the spherical droplet, $T_r=0.7$.

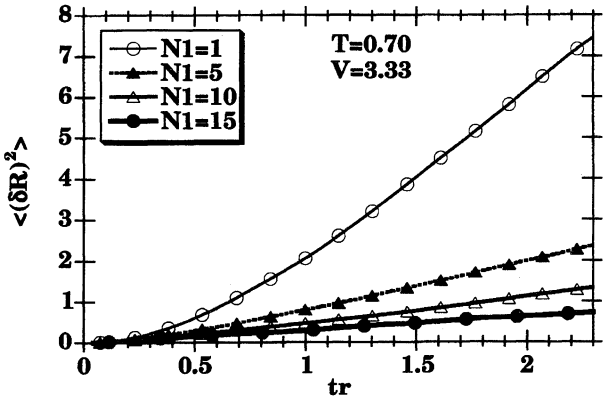

Fig. 20. The mean square displacement of the molecule classified by means of the first coordination number $N1$ at $T_r=0.7$ and $V_r=3.33$.

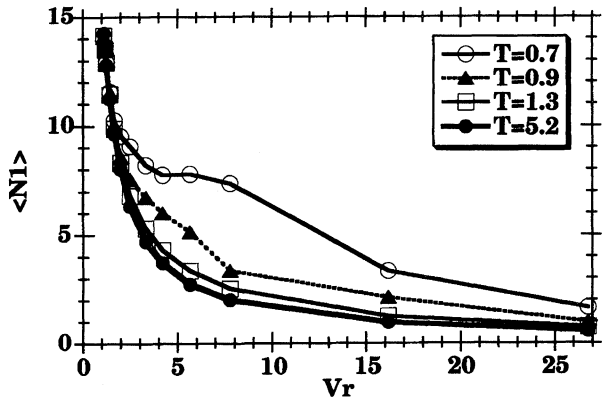

Fig. 21. The average first coordination number $\langle N1\rangle$ is plotted as a function of the volume V_r at several temperatures T_r.

tion of the volume of the hole. The total sum is about 800 close to the volume of the unit cell. It is seen that the large holes appear only at low temperatures (0.70).

In Fig. 15, the running sum $g(V_h)$ is shown at a low temperature (0.70) for several volumes. It is seen that the total sum is only 50% of the volume of the unit cell at volume $V_r=3.33$, which is close to the critical volume $V_{cr}=2.9$. The percentage is 80% at $V_r=5.67$ and 90% at $V_r=7.78$. At $V_r=16.16$ and 26.77, these are larger than 100%. It is possible by the present method to calculate the volume of the hole. An example is the configuration where molecules sit only near the corners of the unit cell. In this case the diameter of the hole is about the body diagonal of the unit cell. The existence of the large holes at $V_r=16.16$ and 26.77 is consistent with the distribution of the cluster size in Fig. 13, which suggests a significant phase separation at low density.

Distribution of the First Coordination Number. Next the molecular environment in the neighborhood will be studied. The number of the molecules within the distance less than 1.6σ is called the first coordination number $N1$. The distribution functions $F(N1)$ are compared at high (5.2), around critical (1.3) and low (0.7) temperatures in Figs. 16, 17, and 18, respectively. It is shown that the distribution depends strongly on the volume.

At volume $V_r=1.25$, the distribution $F(N1)$ always has its peak at 13 in Figs. 16, 17, and 18. This density corresponds to the normal liquid. The distribution becomes sharp at lower temperatures. In the case of low density ($V_r=26.77$), the peak is at 0 even at lowest temperature 0.70, as expected in gas state.

In contrast to this, a large change in the distribution is observed in the medium density ($V_r=3.33$ and 7.78). The distribution $F(N1)$ in a spherical droplet is shown in Fig. 19 for comparison. This is calculated by a spherical sample that is cut from a liquid configuration at low temperature. The two peaks in this distribution are the result of the finite size of the spherical droplet. The peak around 13 comes from the molecules in the inside part of the sphere. The other corresponds to those at the outside part. The distribution at low temperature (0.7) in the medium density is similar to that in Fig. 19. The case of $V_r=7.78$ is assigned to be a mixture of one or two droplets and a few gas-like molecules. In the case of $V_r=3.33$, the size of the droplet-like part is smaller, as seen from ECN in Fig. 11.

It turned out that the phase separation is realized in the medium density at low temperature (0.7). However, we will analyze the states at intermediate temperatures (1.1 and 0.9) and at volumes only a little larger than the liquid state as examples of large density fluctuations in the next section.

Self-Diffusion Coefficient in Large Density Fluctuations

In Figs. 5 and 9, the density dependence of D_r is different at low temperatures (0.7 and 0.9) from that at the other temperatures. This phenomenon will be studied in this section.

Fig. 20 shows the mean square displacement of the molecules that the classified by means of the first coordination number $N1$ at $T_r=0.7$ and $V_r=3.33$. This

means that the self-diffusion coefficients are very different according to the value of $N1$. The average density has a less important meaning to determine the diffusion process of each molecule than $N1$. The distribution of $N1$ is described in Fig. 18.

The average first coordination number $\langle N1 \rangle$ is plotted as a function of the volume V_r at several temperatures in Fig. 21. At a high temperature such as 5.2, $\langle N1 \rangle$ has the value for the case of the random distribution. Even around the critical temperature ($T_{cr}=1.35$) $\langle N1 \rangle$ shows only a small deviation from it. At lower temperatures, 0.9 and 0.7, it deviates as shown in Fig. 21. The volume dependence of $\langle N1 \rangle$ resembles that of D_r shown in Fig. 5. When a liquid sample is expanded, the quantities D_r and $\langle N1 \rangle$ have a step as a function of volume. It is most clearly seen at lowest temperature (0.7). Fig. 21 shows that the decay of $\langle N1 \rangle$ is moderate, compared to the decay of the average density. The self-diffusion coefficient D_r does not increases so steeply as the volume increases around the medium volume at low temperatures (0.7 and 0.9) in Fig. 5 for this reason.

The self-diffusion coefficient D is mainly determined by the average first coordination number $\langle N1 \rangle$, which is determined by the distribution $F(N1)$ of the coordination number $N1$. When the sample has large fluctuations in density, this distribution is important to understand the volume and temperature dependence of D.

The authors would like to thank Professor Hideo Nishiumi for valuable discussions. This work has been supported in part by a Grant-in-Aid for Scientific Research No. 05303006 from the Ministry of Education, Science and Culture. The authors thank the Computer Center of the Institute for Molecular Science for the use of computers. The computation was also done at Computer Center, Hosei University.

References

1) M. P. Allen and D. J. Tildesley, "Computer Simulation of Liquids," Oxford Univ. Press, Oxford (1987).
2) I. R. McDonald and K. Singer, *Mol. Phys.*, **23**, 29 (1972).
3) D. J. Adams, *Mol. Phys.*, **37**, 211 (1979).
4) J. J. Nicolas, K. E. Gubbins, W. B. Street, and D. J. Tildesley, *Mol. Phys.*, **37**, 1429 (1979).
5) F. H. Ree, *J. Chem. Phys.*, **73**, 5401 (1980).
6) Y. Adachi, I. Fijihara, M. Takamiya, and K. Nakanishi, *Fluid Phase Equilib.*, **39**, 1 (1988).
7) K. D. Timmerhaus and H. G. Drickamer, *J. Chem. Phys.*, **19**, 1242 (1951).
8) W. L. Robb and H. G. Drickamer, *J. Chem. Phys.*, **19**, 1504 (1951).
9) A. J. Easteal, *AIChE J.*, **30**, 641 (1984).
10) R. C. Reid, J. M. Prausnitz, and B. E. Poling, "The Properties of Gases and Liquids," 4th ed, McGraw-Hill, New York (1987), p. 577.
11) P. D. Neufeld, A. R. Janzen, and R. A. Aziz, *J. Chem. Phys.*, **57**, 1100 (1972).
12) S. Nosé, *Mol. Phys.*, **52**, 255 (1984).
13) S. Nosé, *J. Chem. Phys.*, **81**, 511 (1984).
14) D. Levesque and L. Verlet, *Phys. Rev. Sect. A*, **A2**, 2514 (1970).